CHARGE TRANSFER ANALYSIS IN TWO-PHASE STEP OXIDE CHARGE COUPLED DEVICE

C.H. CHAN* and S.G. CHAMBERLAIN**

ABSTRACT

Charge transfer phenomenon in charge-coupled devices is characterized by a nonlinear partial differential equation of the parabolic type, usually coupled with a very undesirable nonlinear boundary condition. In this study, special treatment is made to the boundaries such that the nonlinearity of the boundary condition does not appear in the final calculation. Using the linearized Crank-Nicolson scheme (ref 11) the charge transfer phenomenon of a two phase overlapping gate CCD has been studied and numerical results are presented. Special emphasis is directed toward the relative importance of the self-induced drift, fringing field drift and thermal diffusion currents. Also, the usefulness of approximating a spatial fringing field pattern by a constant value to the charge transfer phenomenon is discussed.

I. INTRODUCTION

Charge transfer phenomenon in CCD (ref 1) has been studied by many authors (ref 2-9). In all these studies, it is required to solve the nonlinear continuity equation for the carrier concentration. In their earliest paper, Engeler et al (ref 2) solved the continuity equation with only one term in the current density equation, namely, the gradient-induced, or self-induced drift. Thermal diffusion and self-induced drift were considered simultaneously in the equation by Strain and Schryer (ref 3) and also independently by Kim and Lenzlinger (ref 4). All of these authors had ignored the most important, perhaps, the most difficult term, the fringing field drift. Amelio (ref 5) in his computer modeling, used an effective velocity approach in solving the complete equation with small initial charge. However, this approach underestimates the self-induced drift and results in a longer transfer time. Using a constant value for the fringing field, Heller et al (ref 6) have also solved the complete equation. It is shown in Section III that, using a constant value instead of the exact pattern for the fringing field has a very pronounced effect on the transfer characteristic. Carnes et al (ref 7) and Mohsen et al (ref 8) gave a more complete analysis on the three phase and two phase structure respectively, both using exact fringing field pattern from the solution of the two-dimensional Poisson Equation.

In Section II, the current density equation and the continuity equation are described briefly together with the boundary and initial conditions pertinent to the physical phenomena. A nonlinear boundary condition is encountered when all the three terms; the self-induced drift, fringing field drift and thermal diffusion are considered simultaneously

** With the Department of Electrical Engineering, University of Waterloo, Waterloo, Ontario, Canada.

* Presently with Bell-Northern Research, Ottawa, Ontario, Canada.

in the continuity equation. A treatment is made to the boundaries such that the nonlinearity of the boundary condition does not appear in the final calculation.

Numerical results using various finite-difference schemes for the charge transfer phenomenon where studied and compared in (ref 11). The linearized Crank-Nicolson scheme which was found to be superior to other available schemes was used here for the charge transfer analysis of a two phase overlapping gate CCD. The relative importance of the various constituents of the current density is discussed and emphasis is made on the more difficult to analyse but yet the most influential fringing field drift. Conclusions are made and presented in section IV.

II FORMULATION

The Nonlinear Continuity Equation

It is generally accepted that the flow of the minority carriers along the Silicon surface in a MOS system can be treated as a one-dimensional problem with the current density given by;

$$J = J_y = q(\mu E p - D \frac{\partial p}{\partial y}) \tag{1}$$

where y is the direction of flow parallel to the semiconductor surface; q, the electronic charge; μ, the mobility of minority carrier (in this case, holes for n-substrate devices); E, the total electric field along the surface; p, the hole concentration at the surface and D, the diffusion constant. Assuming that the total electric field can be expressed by the sum of two terms; E_f, the fringing field and E_s, the self-induced field.

$$E = E_f + E_s \tag{2}$$

The fringing field can only be obtained through the solution of the two-dimensional Poisson Equation subject to the appropriate boundary conditions. Methods for obtaining E_f have been reported elsewhere (ref 5, 8, 10, 15) and will not be repeated here. The typical solutions for the surface potential V_s and the fringing field E_f of a two phase overlapping gate CCD at two different doping levels are shown in Fig. 1. The dimensions used for a single bit are also shown in the top of Fig. 1(a).

A one-dimensional linear approximation between the surface potential V_s and surface charge concentration has been widely used (ref 2-4), thus,

$$V_s = V_{so} + \gamma' \, qp/C_{ox} \tag{3}$$

where V_{so} is the surface potential at zero surface charge; γ', a constant determined by the applied voltage, equilibrium surface potential and V_{so}; and C_{ox} is the oxide capacitance per unit area. Taking the negative gradient of V_s, the self-induced field can therefore be written as

$$E_s = - \frac{\partial V_s}{\partial y} = - \gamma' \frac{q}{C_{ox}} \frac{\partial p}{\partial y} \equiv - \gamma \frac{\partial p}{\partial y} \tag{4}$$

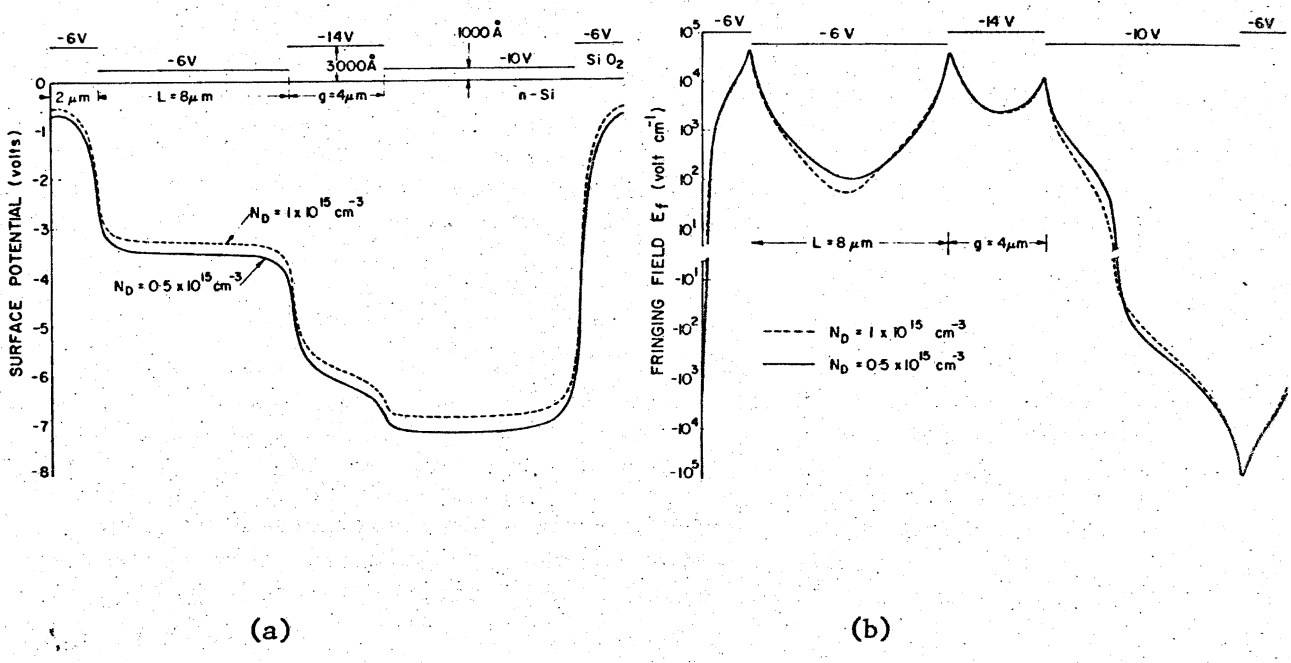

(a) (b)

Fig. 1 The surface potential (a) and fringing field (b) along the semiconductor surface of a two phase overlapping gate CCD for two substrate doping levels. The dimensions of one bit of the device is shown in the top of figure (a).

consequently, (1) can be rewritten as

$$J = q[\mu E_f p - (\gamma\mu + D) \frac{\partial p}{\partial y}] \tag{5}$$

Together with the continuity equation

$$\frac{\partial p}{\partial t} = - \nabla \cdot (\frac{1}{q} J) = - \frac{1}{q} \frac{\partial J}{\partial y}$$

we then have,

$$\frac{\partial p}{\partial t} = \frac{\partial}{\partial y} [(\gamma\mu p + D) \frac{\partial p}{\partial y} - \mu E_f p] \tag{6}$$

Equation (6) relates the time and space dependence of the carrier concentration and is a parabolic equation which in most cases, cannot be solved analytically.

Boundary Conditions and Initial Values

To understand the charge transfer phenomenon in detail, it is necessary to solve equation (6) under the transferring gate region with

the suitable boundary conditions and initial values. Similar to the other existing literature, the boundary conditions and initial values are,

$$J(0,t) = 0 \tag{7}$$

$$p(L,t) = 0 \tag{8}$$

and $$p(y,0) = P_0, \quad 0 \leq y < L \tag{9}$$

where L is the transfer gate length.

Condition (7) implies that an infinite barrier exists to the left edge of the transferring region and ensuring the unidirectional flow of the signal bearing carrier in the device. Condition (8) simulates an infinite sink for the charge carriers to the right edge of the transferring region. Equation (9) is an idealized initial condition, a square wave distribution of minority carrier concentration.

III NUMERICAL RESULTS

Equation (6) has been solved numerically subjected to the boundary and initial conditions (7) - (9) for a two phase overlapping gate CCD using the linearized Crank-Nicolson scheme (ref 11). The fringing field is calculated from the numerical solution of the two-dimensional Poisson Equation and is given in Fig. 1(b). Since the total number of charge carriers under the transferring electrode is of more concern than the spatial carrier concentration distribution, we shall center our attention to the transfer inefficiency defined by;

$$\varepsilon \equiv \frac{\int_o^L p(y,t)dy}{\int_o^L p(y,o)dy} = \frac{1}{LP_o} \int_o^L p(y,t)dy \tag{10}$$

A plot of ε versus normalized time, t/τ_o ($\tau_o \equiv L^2/\mu$), was used here for transfer inefficiency analysis.

Rewriting the current density as

$$J = J_f + J_s + J_d \tag{11}$$

where $$J_f = q\mu E_f p \tag{12}$$

$$J_s = -q\gamma\mu p \frac{\partial p}{\partial y} \tag{13}$$

$$J_d = - qD \frac{\partial p}{\partial y} \tag{14}$$

The last three equations represent the current densities contributed by the fringing field drift, self-induced drift and thermal diffusion respectively. Analytic solution of the continuity equation with only two terms in (6) has been reported (ref 5, 7) and based on a charge-control model and a constant fringing field approximation, transfer efficiency has been successfully expressed in closed form (ref 9). However, it is still of interest to examine the relative importance of the various terms and their contribution toward the charge transfer inefficiency. Fig. 2 shows the result of transfer inefficiencies versus time for all the possible combination of the three terms. It is clearly shown that the

thermal diffusion process is the slowest of the three, and self-induced drift has the most pronounced effect for the first few τ_o but becoming diffusion-like (slow) when more than 90% of the charge have been transferred. Therefore, the combined effect of self-induced drift and diffusion is essentially a diffusion problem with a concentration dependent diffusion coefficient as suggested by Kim (ref 4).

Fringing field drift is slow at the beginning but becoming increasingly fast after a few τ_o. And the combined effect of fringing field drift and diffusion results in an exponential behavior. As a consequence, the total effect of all three terms in the charge transfer should first behave like self-induced drift, then, a combined fringing field and self-induced drift, finally, it becomes a combined fringing field drift and diffusion process.

To examine the self-induced drift more closely, the transfer characteristics for different values of initial carrier concentrations have been obtained and are shown in Fig. 3. The influence of the self-induced drift seems to be weaker progressively with decreasing amount of initial carrier concentration. But the final decay rate (characterized

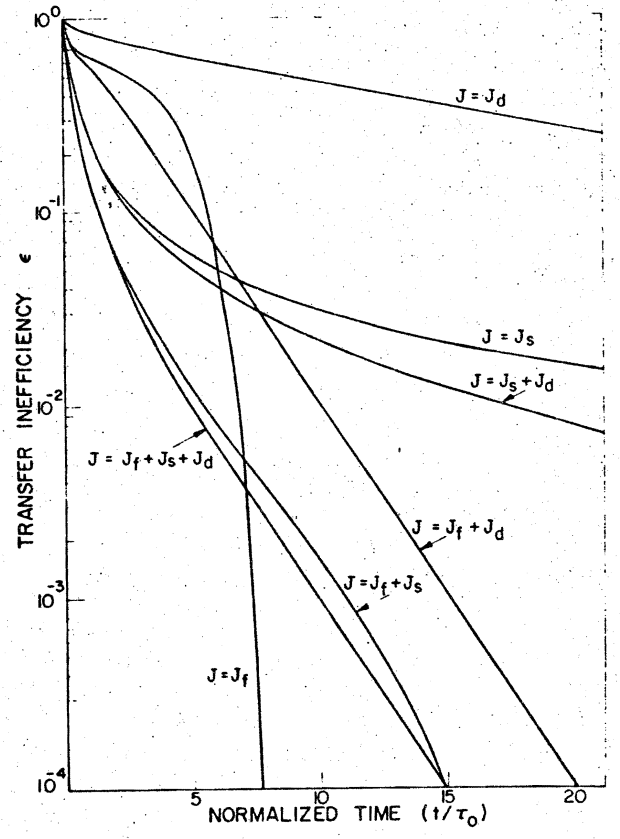

Fig. 2 Relative importance of the three terms, J_f, J_s and J_d in Equation (6).

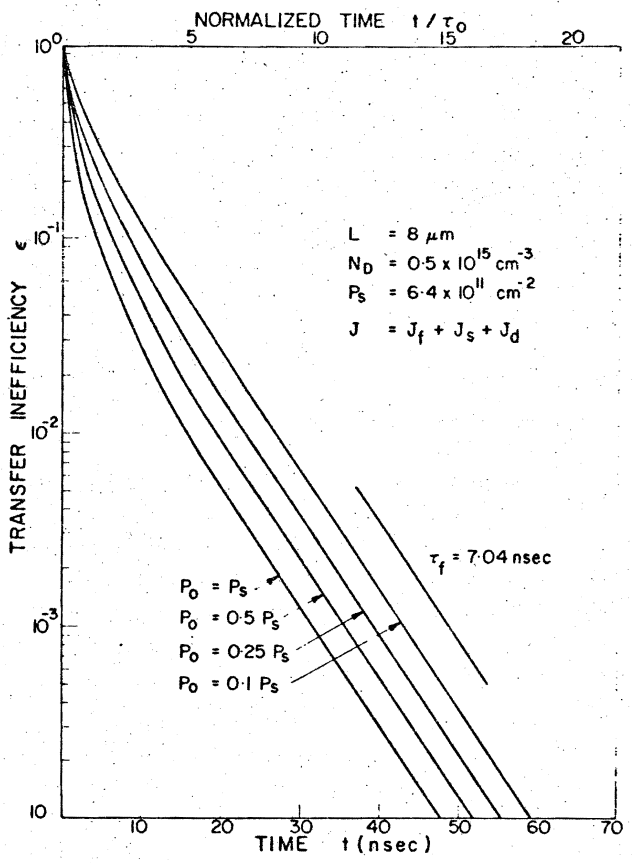

Fig. 3 Transfer characteristics at four different initial carrier concentrations.

by the final decay time constant τ_f) is independent of initial carrier concentration indicating the strong fringing field drift and thermal diffusion for the final stage of decay. The time when combined fringing field drift and thermal diffusion dominate occurs at and around a point

where the average carrier concentration

$$P_{ave} \equiv \frac{1}{L} \int_{o}^{L} p(y,t)dy = 0.01\ P_s \qquad (15)$$

where P_s is the saturated carrier concentration; i.e., when $\varepsilon = 0.01$ for $P_o = P_s$ and $\varepsilon = 0.1$ for $P_o = 0.1\ P_s$.

Fig. 4 shows the transfer characteristics with E_f, the fringing field as a parameter. It is clearly shown, that using $E_f = E_{fmin}$ throughout the transfer region results in a transfer curve not much different from that without the fringing field (E_f=0). The exact pattern of fringing field as calculated has a much faster decay (an average factor of 2). As to the beginning of the transfer, the strong fringing field at the edges of the transfer region causes a higher concentration gradient, hence a higher self-induced field, resulting in a much faster transfer at the beginning.

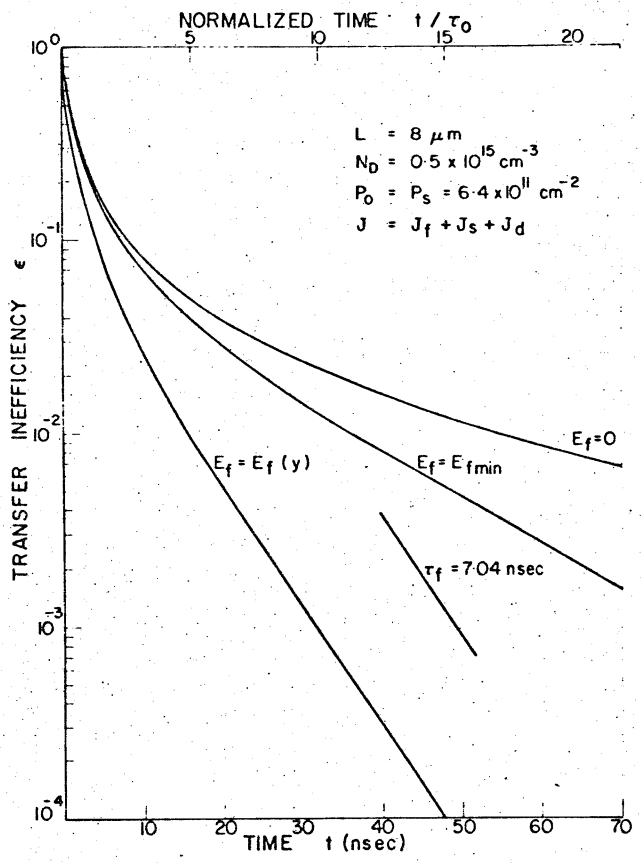

Fig. 4 The influence of the fringing field value on the transfer characteristic. $E_f(y)$ is the fringing field pattern as calculated.

To further examine the importance of the fringing field, the transfer characteristics of two different substrate dopings are shown in Fig. 5 and the corresponding fringing field patterns are shown in Fig. 1(b). The two curves shown differ only by the final stage of decay, where higher substrate doping density results in lower values of fringing fields, hence a slower transfer. Fig. 6 shows the transfer curves for three different transfer gate lengths and the corresponding fringing field patterns (only under the transfer gate region) are shown in Fig. 7. It is shown that, the shorter the transfer region, the deeper the fringing field can penetrate and results in a faster transfer. (Note that the time scale is normalized to τ_o which is proportional to the square of the gate length L).

To give a general idea of how the carriers decay, the spatial distribution of the carrier concentration at various instants are shown in Fig. 8, and Fig. 9 shows the spatial variations of the current density and its constituents at two different times.

Comparing the results obtained to the existing literature, close resemblance is found to those reported on similar structures, but slower transfer rate than those reported in (ref 7) for a three phase structure. The principal difference must be coming from the difference in fringing field patterns for different structure used. Following the same terminology used in (ref 7), the final decay time constant τ_f is given by $(0.45 \pm 0.05)\tau_{tr}$ and t_4, the time to achieve $\varepsilon = 10^{-4}$ is given by $(3.1 \pm 0.05)\tau_{tr}$, where τ_{tr} is the single carrier transit time defined by

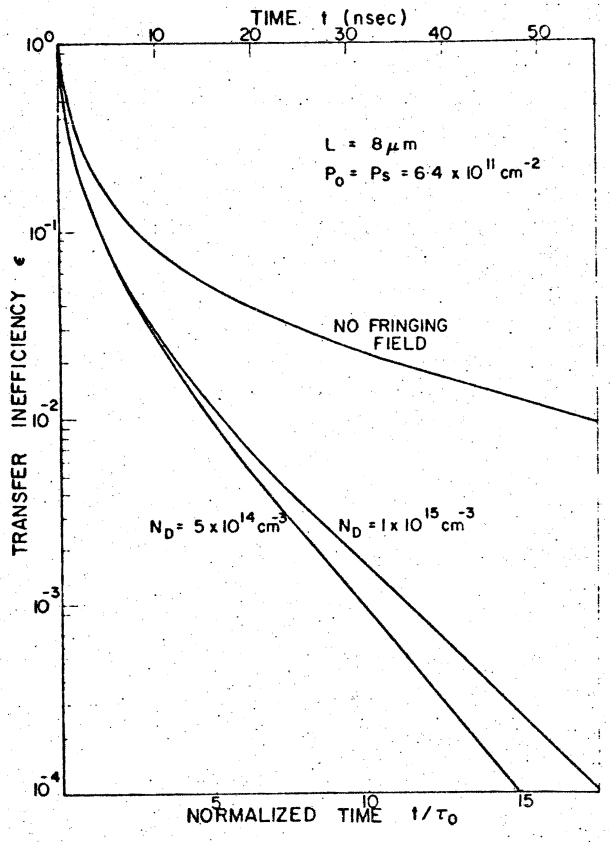

Fig. 5 Transfer characteristics at two different substrate doping levels.

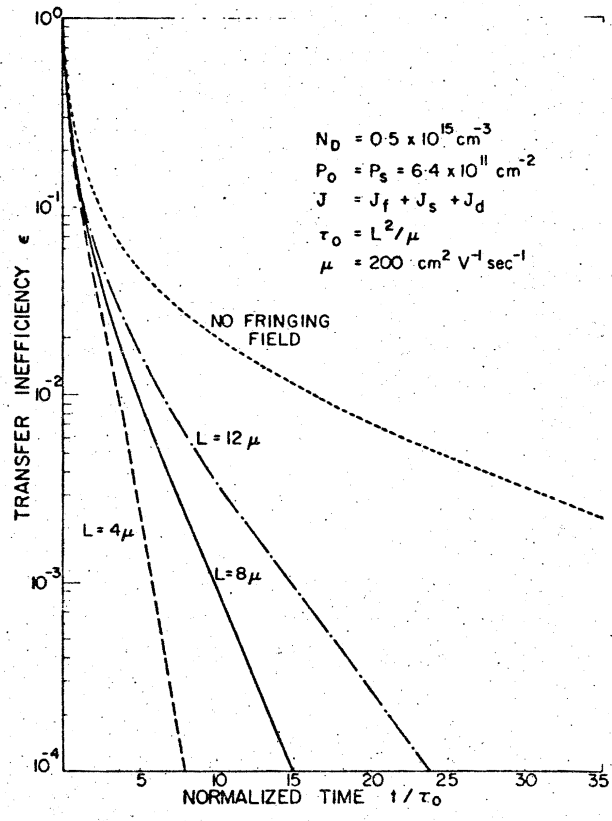

Fig. 6 Transfer inefficiency versus normalized time for three different gate lengths.

$$\tau_{tr} \equiv \frac{1}{\mu} \int_o^L \frac{dy}{E_f(y)}.$$

IV SUMMARY AND CONCLUSION

Charge transfer under a transferring electrode in a CCD structure is characterized by the three current density components, the self-induced drift, the fringing field drift and thermal diffusion. The resulting continuity equation that describe the transfer phenomenon is a nonlinear parabolic equation (Equation (6)). The pertinent boundary and initial conditions are given by Equations (7) through (9).

Numerical results of a two phase overlapping gate CCD using the Linearized Crank-Nicolson Scheme have been presented. Each component in the current density equation has been examined separately and their relative importance have been discussed. It is concluded that the charge transfer is first initiated by the self-induced field and the high fringing field at the edges of the transfer region. As the transfer process proceeds, the former weaken faster than the latter until a point whereby the remaining carrier concentration falls below a few percent of its saturated value (determined by the oxide thickness, substrate doping and the applied gate voltage of the device), the former diminishes, leaving behind the fringing field drift and thermal diffusion as the governing transfer mechanisms.

It has also been shown that approximating the exact fringing field pattern by its minimum value results in a two to three fold over-

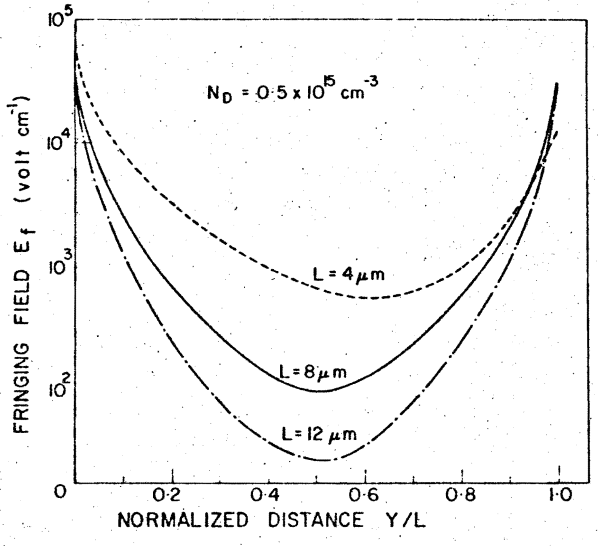

Fig.7 Fringing field pattern under the transfer gate for three different gate lengths. $N_D = 0.5 \times 10^{15}$ cm^{-3}.

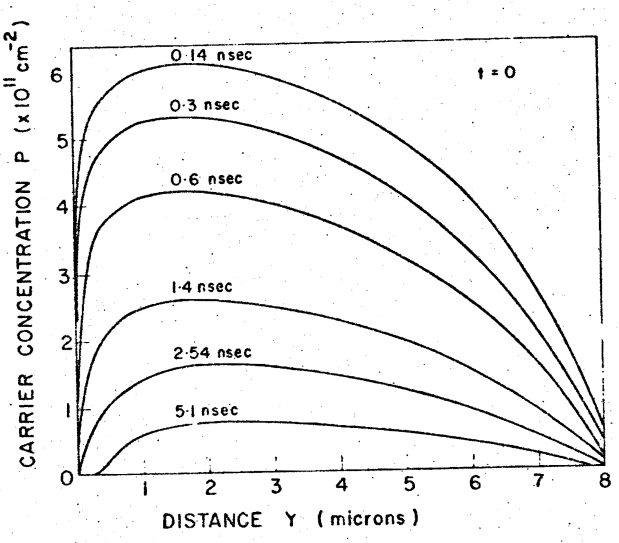

Fig.8 Carrier concentration distribution under the transfer gate at various t.

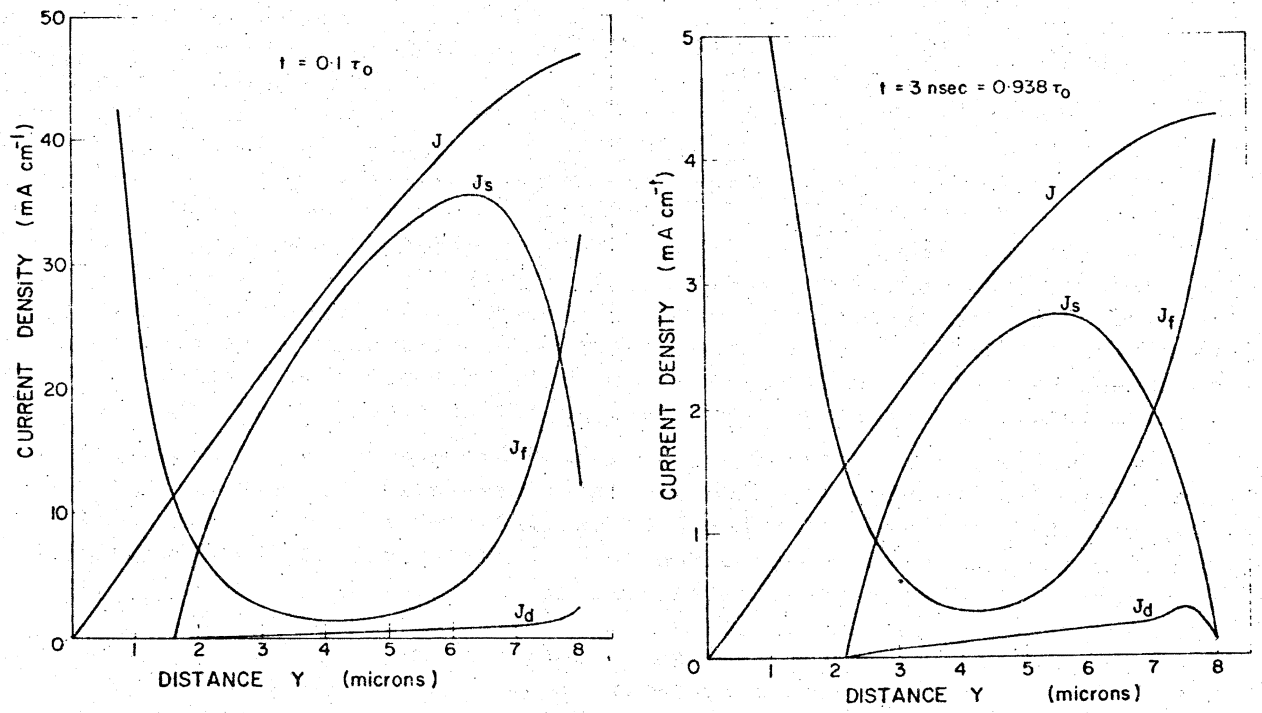

(a) (b)

Fig.9(a) Spatial variations of the total current density J and its three components at (a) $t = 0.1\ \tau_o$ and (b) $t = 0.938\ \tau_o$.

estimate on the transfer time required to reach a certain transfer efficiency. Therefore, accurate estimate on transfer characteristic cannot be obtained unless through the use of an exact fringing field pattern. Results of Figures 6 and 7 also infer the fact that smaller transfer gate length results in larger fringing field, hence a faster transfer. From the free-charge transfer point of view, it is therefore suggested that when high transfer efficiency is required, high fringing field is desirable and can be obtained by optimizing the device structure through the variations of oxide thicknesses, gate lengths and the substrate doping. However, although not discussed here, the fast interface-state trapping (ref 12-15) which also affects the charge transfer efficiency, should also be considered for optimum CCD circuit design.

ACKNOWLEDGEMENT

This work was carried out at the University of Waterloo and supported in part by National Research Council of Canada, grant Number A7384.

REFERENCES

1. W.S. Boyle and G.E. Smith, Bell Syst. Tech. J., 49, 587(1970).

2. W.E. Engeler, J.J. Tiemann and R.D. Baertsch, Appl. Phys. Lett., 17, 469(1970).

3. R.J. Strain and N.L. Schryer, Bell Syst. Tech. J., 50, 1721(1971).

4. C. Kim and M. Lenzlinger, J. Appl. Phys., 42, 3586(1971).

5. G.F. Amelio, Bell Syst. Tech. J., 51, 705(1972).

6. L.G. Heller, W.H. Chang and A.W. Lo, IBM J. Res.Dev., March. 184(1972).

7. J.E. Carnes, W.F. Kosonocky and E.G. Ramberg, IEEE Trans. Elect. Dev., ED-19, 798(1972).

8. A.M. Mohsen, T.C. McGill and C.A. Mead, IEEE J. Solid-State Circuits, SC-8, 191(1973).

9. H. Lee and L.G. Heller, IEEE Trans. Elect. Dev.,ED-19,1270(1972).

10. W.H. Chang, Solid-State Elect., 16, 491(1973).

11. C.H. Chan and S.G. Chamberlain, Solid-State Elect.,17,491(1974).

12. M.F. Tompsett, IEEE Trans. Elect. Dev., ED-20, 45(1973).

13. J.E. Carnes and W.F. Kosonocky, Appl. Phys. Lett., 20,261(1972).

14. A.M. Mohsen, T.C. McGill, Y. Daimon and C.A.Mead, IEEE, J.Solid-State Circuits, SC-8, 125(1973).

15. J. McKenna and N.L. Schryer, Bell Syst. Tech. J., 52, 669(1973).